Registration Uncertainty for Robot Self-localization in 3D

Pifu Zhang
Faculty of Computer Science
Dalhousie University
pifu@cs.dal.ca

Jason Gu
Dep. of Electrical & Computer Engi.
Dalhousie University
jason.gu@dal.ca

Evangelos E. Milios
Faculty of Computer Science
Dalhousie University
eem@cs.dal.ca

Abstract

Stereo camera is a very important sensor for mobile robot localization and mapping. Its consecutive images can be used to estimate the location of the robot with respect to its environment. This estimate will be fused with location estimates from other sensors for a globally optimal location estimate. In the data fusion context, it is important to compute the uncertainty of the stereo-based localization. In this paper, we propose an approach to obtain the uncertainty of localization when a correspondence-based method is used to estimate the robot pose. The computational complexity of this approach is $O(n)$, where n is the number of corresponding image points. Experimental results shows that this approach is promising.

Keywords: localization, error propagation, uncertainty, registration.

1 Introduction

Simultaneous localization and mapping (SLAM) for autonomous robots is still a challenge, especially in outdoor 3D environment. More and more systems are equipped with many sensors, such as stereo camera, inertial navigation sensor (INS), laser range finder, global positioning system (GPS), to implement their goal. Appropriate sensor fusion methods will be used to integrate the measurements from all the sensors on the robot to obtain a globally optimized solution. As a very important and frequently used sensor, stereo camera can provide a full view of environment, and also self-localization information. Generally, the self-localization algorithm can be classified as correspondence-based and flow-based. In the correspondence-based method, a set of 3D points is obtained from each robot position. Self-localization requires the establishment of correspondence and registration between sets of 3D points from consecutive robot positions. But the localization from the registration cannot be directly used for the sensor fusion, because the uncertainty of the localization is required in addition.

In this paper, we present an approach to calculate the self-localization uncertainty which is suitable for the correspondence-based method. This approach uses the error propagation theory based on the implicit function theorem. Robot navigation experiment is implemented to show the uncertainty of its location.

2 Previous Work

Approaches for extracting motion information from image sequences can be classified as *correspondence-based* and *flow-based*. Correspondence methods [17, 9] track distinct features such as corner, line, high curvature point, SIFT, etc., through the image sequence and compute 3D structure by triangulation. Flow-based methods [3, 21] treat the image sequence as function $f(x, y, t)$, where (x, y) are image pixel coordinates and t is time, restrict the motion between frames to be small, and compute shape and motion in terms of differential changes in the function f.

In the correspondence-based method, the most important step is to register the two sets of data according to the correspondence. Once we obtain

the estimate registration values, we face the question that how precise is it.

Lowe [13] used least-squares minimization procedure to obtain the robot pose as well as its covariance. Based on this method, Se, Lowe and Little [19] presented a method for mobile robot localization and mapping with uncertainty by fusion of robot odometry information and visual estimation information with Kalman filter. Davison [5] also used Kalman filter to solve the robot pose and its uncertainty problem with a single camera.

Another way to estimate robot pose uncertainty is statistical analysis method which is based on the implicit function theorem [6, 3]. Jokinen [12] used this method to derive more general strategies to analyze the propagation of measurement and calibration errors to the registration parameters and further to the reconstructed model of the scene consisting of planar patches. Ma,et al [16] addressed the issues of sensitivity and robustness in their motion recovery algorithm from the image velocities. Sun, et al [20] have proposed an error characterization of the factorization method for 3-D shape and motion recovery from image sequences using matrix perturbation theory. All of the methods are used in the application area of flow-based.

In this paper, we develop a procedure for estimating the uncertainty of the robot pose obtained via a correspondence-based method. Our method uses the implicit function theorem to derive the pose uncertainty from a maximum likelihood formulation, which has a similar idea as the above flow-based method.

The accuracy analysis of the estimated location by using statistical method for the robot self-localization based on stereo vision is the main contribution in this paper. The paper is organized as follows. In section 3, we briefly introduce the method to estimate the self-localization from the stereo images. In section 4, we present an approach to calculate the registration parameter's accuracy based on the implicit function theorem and Taylor formula. In section 5, we implement experiment for the uncertainty analysis of robot navigation. In the last section, we present a summary of our proposal and conclusions.

3 Self-localization Estimation via Stereo

With the stereo camera system, it is possible to get a rectified image(the distortion in the original image has been modified) I_t and a 3D cloud C_t at time t, for all t. From the image I_t, we can extract a set of SIFT (Scale Invariant Feature Transform) features [14] F_t^i, $(i = 1, \cdots, N_t)$. In the sequence of images, SIFT feature correspondence can be established between any two adjacent images. RANSAC method [8] is implemented to delete the outliers in the previous initial matching. For any matched feature, its 3D point could be obtained from the associated 3D cloud. Since the SIFT feature gives a sub-pixel position in the image, it is necessary to use bilinear interpolation to obtain an accurate 3D position. So it is possible to obtain, for a 3D point M_t^i in C_t, a corresponding 3D point $M_{t-1}^i \in R^3, i = 1, \ldots, n$, in C_{t-1}. Since the two data sets are derived from different image frames, their covariance will be changed with the image's depth. Therefore, the corresponding points will have different error covariance. We assume that the error for every point i at time t can be expressed as $\sigma_{M_t^i}$ (see Appendix B).

In order to obtain the self-localization information between time step $t-1$ and t, we can directly register the cloud C_{t-1} to cloud C_t by using the corresponding data M_{t-1}^i and M_t^i. Gaussian based maximum likelihood (ML) method can be used for this problem [1, 17]. The maximum-likelihood estimate for rotation R (since q is a quaternion of rotation, q and R will be used for rotation when it is required) and translation T is obtained by minimizing the following objective function

$$\min_{R,T} \quad E(R,T) = \sum_{i=1}^{n} \nu_i' S_i^{-1} \nu_i \tag{1}$$

where $\nu_i = M_t^i - RM_{t-1}^i - T$ is called innovation, and $S_i = R\sigma_{M_{t-1}^i} R' + \sigma_{M_t^i}$ is its associated covariance.

Before the registration process, we can obtain the centroid of the two sets of data as $M_t^c = \sum_{i=1}^n M_t^i/n$ and $M_{t-1}^c = \sum_{i=1}^n M_{t-1}^i/n$. By subtracting the centroid from each point, we obtain two new data sets $\hat{M}_t^i = M_t^i - M_t^c$ and $\hat{M}_{t-1}^i = M_{t-1}^i - M_{t-1}^c$. Substituting the new data sets $\hat{M}_t^i$ and $\hat{M}_{t-1}^i$ into in the innovation ν_i, the objective function (1) can be

changed to

$$min \quad E = \sum_{i=1}^{n} (\hat{M}_t^i - R\hat{M}_{t-1}^i)' S_i^{-1} (\hat{M}_t^i - R\hat{M}_{t-1}^i) \tag{2}$$

This is a non-linear function, and we solve this optimization problem through linearization and iteration, which was applied by Lu and Milios [15] and Olson et al [18]. To make it simple, we express the rotation R in the form of quaternion $R = R(q)$ and $q = (q_0, q_1, q_2, q_3)$. We linearize the problem by taking the first-order expansion with respect to the rotation in the quaternion expression. Let q^0 be the initial rotation estimates and R_0 be the corresponding rotation matrix. The first-order expansion is:

$$E = \sum_{i=1}^{n} (G_t^i - J_t^i q)' S_i^{-1} (G_t^i - J_t^i q) \tag{3}$$

where $J_t^i = [\frac{\partial R}{\partial q_0}\hat{M}_{t-1}^i, \frac{\partial R}{\partial q_1}\hat{M}_{t-1}^i, \frac{\partial R}{\partial q_2}\hat{M}_{t-1}^i, \frac{\partial R}{\partial q_3}\hat{M}_{t-1}^i]$ (see Appendix A), and $G_t^i = \hat{M}_t^i - R_0\hat{M}_{t-1}^i - J_t^i q^0$. Differentiating the objective function with respect to q and setting the derivatives to zero yields:

$$q = (\sum_{i=1}^{n} J_t^{i\prime} S_i^{-1} J_t^i)^{-1} \sum_{i=1}^{n} (J_t^{i\prime} S_i^{-1} G_t^i) \tag{4}$$

After solving (4), this estimated rotation is used as an initial estimate of the next step, and the process is iterated until it converges. Then the translation can be obtained by

$$T = RM_{t-1}^c - M_t^c \tag{5}$$

4 Uncertainty of Localization Estimate

During the registration step, we obtain the robot pose: rotation q and translation T. But what is the reliability of this estimate? From the objective function (3) we knew that the rotation q and the measurement M $(= [M_{t-1}^i, M_t^{i\prime})$, $(i = 1, \ldots, N)$ are related through an implicit function.

$$\Psi(q, M) = 0 \tag{6}$$

According to the implicit function theorem [6, 7], there has

$$\frac{\partial q}{\partial M} = -(\frac{\partial \Psi}{\partial q})^{-1} \frac{\partial \Psi}{\partial M} \tag{7}$$

We express the rotation as a function of the measurements

$$q = f(M) \tag{8}$$

Expanding f in a Taylor series around $E[M]$ yields

$$f(M) = f(E[M]) + (M - E[M]) \frac{\partial q}{\partial M} + O(M - E[M])^2 \tag{9}$$

where $O(.)^2$ denotes terms of order 2 or higher in M and $\frac{\partial q}{\partial M}$. Up to a first-order approximation, then the covariance of q can be obtained as

$$\sigma_q = \frac{\partial q}{\partial M} \sigma_M (\frac{\partial q}{\partial M})' \tag{10}$$

If we define $\Phi = \frac{\partial E'}{\partial q}$, then there will have

$$\frac{\partial \Phi}{\partial q} = \frac{\partial^2 E}{\partial q^2} \quad and \quad \frac{\partial \Phi}{\partial M} = \frac{\partial^2 E}{\partial M \partial q} \tag{11}$$

Substituting equation (11) into equation (10), the covariance σ_q will be

$$\sigma_q = (\frac{\partial^2 E}{\partial q^2})^{-1} (\frac{\partial^2 E}{\partial M \partial q}) \sigma_M (\frac{\partial^2 E}{\partial M \partial q})' (\frac{\partial^2 E}{\partial q^2})'^{-1} \tag{12}$$

From the definition of the objective function (Eq.(3)), we have

$$\frac{\partial E}{\partial q} = \sum_{i=1}^{n} (-\frac{\partial R}{\partial q}\hat{M}_{t-1}^i)' S_i^{-1} (\hat{M}_t^i - R\hat{M}_{t-1}^i) \tag{13}$$

$$\begin{aligned} \frac{\partial^2 E}{\partial q_s \partial q_t} = \sum_{i=1}^{n} \Big[& (-\frac{\partial R^2}{\partial q_s \partial q_t}\hat{M}_{t-1}^i)' S_i^{-1} (\hat{M}_t^i - R\hat{M}_{t-1}^i) \\ & + (\frac{\partial R}{\partial q_s}\hat{M}_{t-1}^i)' S_i^{-1} \frac{\partial R}{\partial q_t}\hat{M}_{t-1}^i \Big] \end{aligned} \tag{14}$$

where s and t equal to $0, 1, 2, 3$.

$$\begin{aligned} \frac{\partial^2 E}{\partial M_{t-1}^i \partial q_s} = & (-\frac{\partial R}{\partial q_s})' S_i^{-1} (\hat{M}_t^i - R\hat{M}_{t-1}^i) \\ & + (\frac{\partial R}{\partial q_s}\hat{M}_{t-1}^i)' S_i^{-1} R \end{aligned} \tag{15}$$

$$\frac{\partial^2 E}{\partial M_t^i \partial q_s} = (-\frac{\partial R}{\partial q_s}\hat{M}_{t-1}^i)' S_i^{-1} \tag{16}$$

$$\frac{\partial^2 E}{\partial M_i \partial q_s} = \begin{pmatrix} \frac{\partial^2 E}{\partial M_{t-1}^i \partial q_s} & \frac{\partial^2 E}{\partial M_t^i \partial q_s} \end{pmatrix} \tag{17}$$

where $i = 1, \cdots, n$ and $s = 0, 1, 2, 3$. Substituting the Eq. (14) and (17) into (12), the covariance of q can be obtained. The covariance for the translation can be calculated by

$$\sigma_T = \sigma_{M_{t-1}}^c + R\sigma_{M_t^c} R' \tag{18}$$

Table 1: Algorithm for 3D data registration and its uncertainty

Input:*two adjacent images I_{t-1} and I_t, and their 3D cloud C_{t-1} and C_t and Image pixel error*
Output: *transformation q, T; variance σ_q, σ_T*
1 *Extract SIFT feature from images I_{t-1}, I_t*
2 *Establish feature correspondences*
3 *Implement RANSAC to delete outliers*
4 *Estimate robot pose by eq. (4) and (5)*
5 *Calculate rotation uncertainty by eq. (12)*
6 *Calculate translation uncertainty by eq. (18)*
7 *output q, T, and σ_q and σ_T*

where $\sigma_{M^c_{t-1}}$ and $\sigma_{M^c_t}$ are the covariance of the center point of data set M_{t-1} and M_t, respectively.

The computational complexity of this algorithm is $O(n)$, where n is the number of corresponding points. The algorithm for the registration of 3D data and its uncertainty estimation is shown in Table 1.

5 Experiment and Analysis

5.1 Lab Experiment

We performed the lab experiment with a BumbleBee camera system mounted on a Mitsubishi PA10-7CE Robot. The robot arm has a maximum speed of 3.33 meters per second and a payload of 10 kilograms (Fig. 1). The camera connects via an IEEE 1394 link to a PC. The stereo camera captures two 320×240 color images when the robot is stationary. Functions of a library provided by the company process the original images and return the associated rectified color images and a list of 3D cloud points associated with of its rectified pixels. Points farther than four meters are discarded during the stereo processing in this test environment.

Figure 1: The Bumblebee stereo camera from Point Grey Research mounted at the tip of the PA10-7CE robot arm.

5.2 Self-localization estimation

During the lab experiment, we did not use any artificial landmarks. The features used in this paper are SIFT features [14], which are extracted from the image in every time step. Two adjacent images are matched for robot self-localization. We used the RANSAC method [8] to delete the outliers. From the matched image points, their associated 3D points could be obtained from the associated 3D cloud. After this processing, we obtain two sets of 3D points which are matched correctly, and then data registration is implemented by the method described in

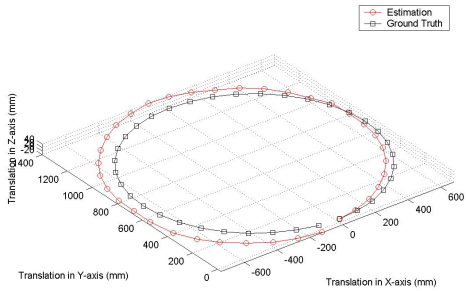

Figure 2: Robot trajectory displayed in 3D in test case 1. Ground truth is obtained by the internal position sensors of the robot arm.

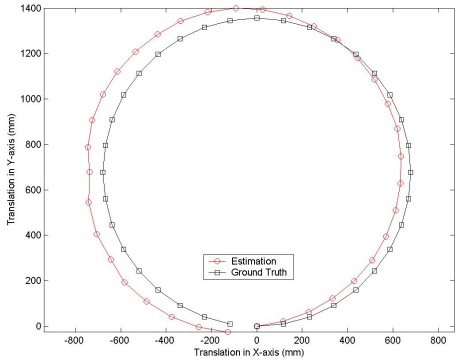

Figure 3: Robot trajectory of Fig. 2 displayed in the horizontal plane (x-y).

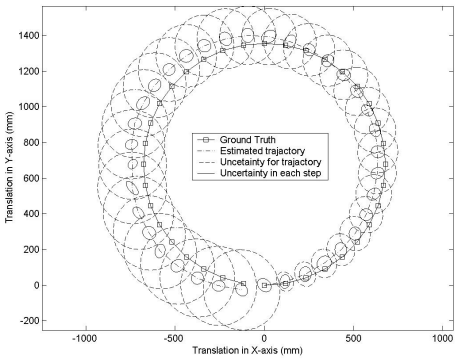

Figure 4: Estimated robot trajectory in x-y plane with associated uncertainty in test case 1

section 3 to get rotation R and translation T. Suppose that the robot's start position is P_0, and the translation at time t is T_t, and rotation is R_t, then the absolute position of the robot can be obtained by

$$P_t = P_{t-1} + R_t * T_t \tag{19}$$

where $t = 1, \cdots, N$, and N is the number of measurements in the circle. The robot's build-in high precision position system provides ground truth of the robot motion trajectory. The estimated trajectory in 3D and 2D on the x-y plane are showed in Fig. 2 and Fig. 3. The image based self-localization estimation is a 6 DOF problem, even though the robot moves in a plane, the estimated trajectory is not planar (Fig. 3) due to the estimation error.

5.3 Uncertainty analysis

By using equations (12) and (18), the uncertainty of robot localization in every step can be obtained together with robot pose estimation. For the rotation, the uncertainty is a 4×4 matrix since the rotation is expressed as quaternion during pose estimation. And the uncertainty of translation is a 3 matrix, which can be expressed graphically with ellipsoid [4]. In our test, we just took the x-y plane to show the estimation uncertainty with the associated ellipse in every robot position. In Fig. 4, the small ellipses are the estimated uncertainty in every robot position. We knew from the results that in every time step, the location uncertainty is almost similar, but its direction changes in different position.

The robot trajectory calculation by Eq.(19) is an iterative process. The uncertainty of absolute position can be calculated as

$$\sigma_{p_t} = \sigma_{p_{t-1}} + R\sigma_{T_t}R' \tag{20}$$

where $t = 1, \cdots, N$ and $\sigma_{p_0} = I_3$, and I_3 is an identical matrix with a dimension of 3. Therefore, the uncertainty of the robot position increase with time. This is displayed in ellipses as shown in Fig. 4. In order to control the uncertainty growth with the time increasing, some techniques, such as Kalman filter, should be used, but it is beyond the scope of this paper.

We present another experimental result shown in Fig. 5. In this case, we took more images in the circular trajectory of the robot arm than in the previous case. The uncertainty in every robot position (small ellipses in Fig. 5) is almost similar to that of Fig. 4, since both of the experiments had the same environment set-up, and used the same camera with the same calibration parameters. But the uncertainty of the robot position is larger than in Fig. 4, because we used more steps to obtain the robot trajectory in this case than in the previous case and this increased the error propagation. As we said, this kind of error propagation can be avoided using Kalman filter.

6 Conclusions

The stereo camera is a very frequently used sensor for autonomous robot localization and mapping. The stereo image will be used to estimated the pose of a robot. This estimation will be fused with other sensor measurements or and associated location estimates in a global optimization framework. Therefore, it is required to provide the uncertainty of the localization for the sensor fusion. For the

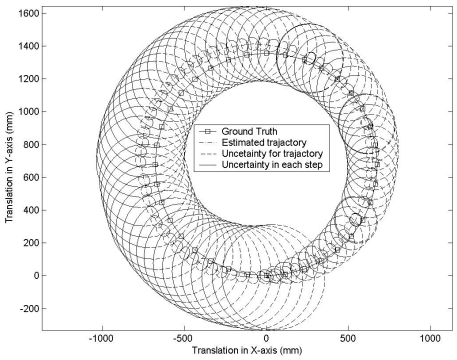

Figure 5: Estimated robot trajectory in x-y plane with associated uncertainty in test case 2, where the density of sampling along the circular trajectory is higher than in test case 1

correspondence-based self-localization estimation method, we propose an approach to obtain the uncertainty of the localization, which is based on the error propagation theory. The computational complexity of this approach is $O(n)$ (where n is the number of corresponding points). Experiment shows that this approach has potential.

Fusing the results from visual camera with other senors to obtain a globally optimized robot localization and map is our next research target for the underwater walking robot. Our method will be compared with the method of Lowe [13] and Se, et al [19].

Acknowledgements: The authors would like to thank Weimin Shen for his help in collecting the image data for our experiments.

Funding for this work was provided by NSERC Canada and IRIS NCE

References

[1] A. Adam, E. Rivlin, and I. Shimshoni. Computing the sensory uncertainty field of a vision-based localization sensor. *IEEE Transactions on Robotics and Automation*, 17:258–267, 2001.

[2] M. J. Brooks, W. Chjnacki, D. Gawley, and A. Hengel. What value covariance information in estimation vision parameters? In *IEEE Proceedings of the ICCV*, 2002.

[3] A. R. Chowdhury and R. Chellappa. Statistical error propagation in 3D modeling from monocular video. *IEEE Workshop on Statistical Analysis in Computer Vision*, 2003.

[4] G. Csurka, C. Zeller, Z. Zhang, and O. Faugeras. Characterizing the uncertainty of the fundamental matrix. In *Techinical report*, INRIA, June 1995.

[5] A. Davison. Real-time simultaneous localisation and mapping with a single camera. In *ICCV2003*, 2003.

[6] O. D. Faugeras. *Three-Dimensional Computer Vision: A Geometric viewpoint.* MIT Press, 1993.

[7] J. Fessler. Mean and variance of implicitly defined biased estimators (such as penealized maximum likelihood): Application to tomography. *IEEE Transaction on Image Processing*, 5:493–506, 1996.

[8] M. A. Fischler and R. C. Bolles. Random sample consensus: a paradigm for model fitting with applications to image analysis and automated cartography. *Communications of the ACM*, 24, 1981.

[9] M. A. Garcia and A. Solanas. 3D simultaneous localization and modeling from stereo vision. In *Proceedings of the 2004 IEEE International Conf. on Robotics and Automation*, pages 847–853, New Orleans, LA, April 2004.

[10] Berthold K. P. Horn. Closed-form solution of absolute orientation using unit quaternions. *Journal of Optical Society of America*, 4:629–642, 1987.

[11] R. Jain, R. Kasturi, and B. G. Schunck. *Machine Vision.* McGraw-Hill, Inc., New York, 1995.

[12] O. Jokinen and H. Haggren. Statistical analysis of two 3-D registration and modeling strategies. *Journal of Photogrammetry and Remote Sensing*, 53:320–341, 1998.

[13] D. G. Lowe. Robust model-based motion tracking through the integration of search and estimation. *International Journal of Computer Vision*, 8:113–122, 1992.

[14] D. G. Lowe. Distinctive image features from scale-invariant keypoints. *International Journal of Computer Vision*, 60:91–110, 2004.

[15] F. Lu and E. Milios. Globally consistent range scan alignment for environment mapping. *Autonomous Robots*, 4(4):333–349, 1997.

[16] Y. Ma, J. Kosecka, and S. Sastry. Linear differential algorithm for motion recovery: A geometric approach. *International Journal of Computer Vision*, 36:343–350, 2000.

[17] L. Matthies and S. A. Shafer. Error modeling in stereo navigation. *IEEE Journal of Robotics and Automotion*, RA-3:239–248, 1987.

[18] C. F. Olson, L. H. Matthies, M. Schoppers, and M. W. Maimone. Stereo ego-motion improvements for robust rover navigation. In *Proceedings of IEEE International Conference on Robotics and Automation*, Korea, May 2001.

[19] S. Se, D. Lowe, and J. Little. Mobile robot localization and mapping with uncertainty using scale-invariant visual landmarks. *Int. Journal of Robotics Research*, 21:735–758, 2003.

[20] Z. Sun, V. Ramesh, and A. M. Tekalp. Error characterization of the factorization method. *Computer Vision and Image Understanding*, 82:110–137, 2001.

[21] G. J. Young and R. Chellappa. Statistical analysis of inherent ambiguities in recovering 3-D motion from a noisy flow field. *IEEE Transactions on Pattern Analysis and Machine Intelligence*, 14:995–1013, 1992.

A Relationship between Rotation Matrix and Quaternion

Quaternion q consists of four components (q_0, q_1, q_2, q_3). It has the following relationship with rotation matrix [10]

$$R = \begin{pmatrix} r_{11} & r_{12} & r_{13} \\ r_{21} & r_{22} & r_{23} \\ r_{31} & r_{32} & r_{33} \end{pmatrix} \tag{21}$$

where $r_{11} = q_0^2 + q_1^2 - q_2^2 - q_3^2$, $r_{12} = 2(q_1q_2 - q_0q_3)$, $r_{13} = 2(q_1q_3 + q_0q_2)$, $r_{21} = 2(q_1q_2 + q_0q_3)$, $r_{22} = q_0^2 - q_1^2 + q_2^2 - q_3^2$, $r_{23} = 2(q_2q_3 - q_0q_1)$, $r_{31} = 2(q_3q_1 - q_0q_2)$, $r_{32} = 2(q_3q_2 + q_0q_1)$, and $r_{33} = q_0^2 - q_1^2 - q_2^2 + q_3^2$. And

$$\frac{\partial R}{\partial q_0} = \begin{pmatrix} 2q_0 & -2q_3 & 2q_2 \\ 2q_3 & 2q_0 & -2q_1 \\ 2q_2 & 2q_1 & 2q_0 \end{pmatrix} \tag{22}$$

$$\frac{\partial R}{\partial q_1} = \begin{pmatrix} 2q_1 & 2q_2 & 2q_3 \\ 2q_2 & -2q_1 & -2q_0 \\ 2q_3 & 2q_0 & -2q_1 \end{pmatrix} \tag{23}$$

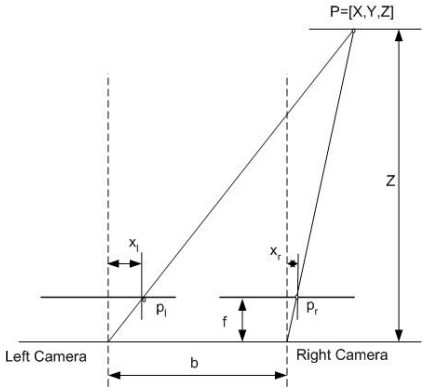

Figure 6: Stereo geometry for triangulation operation[11]

$$\frac{\partial R}{\partial q_2} = \begin{pmatrix} -2q_2 & 2q_1 & 2q_0 \\ 2q_1 & 2q_2 & 2q_3 \\ -2q_0 & 2q_3 & -2q_2 \end{pmatrix} \tag{24}$$

$$\frac{\partial R}{\partial q_3} = \begin{pmatrix} -2q_3 & -2q_0 & 2q_1 \\ 2q_0 & -2q_3 & 2q_2 \\ 2q_1 & 2q_2 & 2q_3 \end{pmatrix} \tag{25}$$

B The Covariance of Estimated 3D Point from Stereo Image

Assume that the measured image coordinates in 2D and inferred 3D points by triangulation from stereo images have normally distributed (Gaussian) error. The Gaussian distribution model to express the error of image coordinates is a common and convenient approximation that will give adequate performance [2]. For the 3D points, the true distribution is a non-Gaussian because triangulation is a non-linear operation [17]. If the distance to the point is not extreme, the Gaussian distribution for 3D is acceptable.

In the properly calibrated stereo system, it is possible to assume that the cameras have parallel image plane, aligned epipolar lines. In Fig. 6 the 3D point $M = [X, Y, Z]$ is observed at points $m_l = [x_l, y_l]$ and $m_r = [x_r, y_r]$ in the left and right image planes, respectively. Without lost of generality, let us assume that the origin of the coordinate system coincides with the left lens center. By using the simple noise-free triangulation operation, we have

$$X = bx_l/(x_l - x_r) \tag{26}$$

$$Y = by_l/(x_l - x_r) \tag{27}$$

$$Z = bf/(x_l - x_r) \tag{28}$$

Due to the error in image coordinates, the covariance for the 3D point $M = f(m_l, m_r)$ will be

$$\sigma_M = J \begin{bmatrix} \sigma_{m_l} & 0 \\ 0 & \sigma_{m_r} \end{bmatrix} J' \tag{29}$$

where J is the matrix of first partial derivatives of f respect to the random vectors m_l and m_r, and is called Jacobian.

$$J = \begin{pmatrix} -bx_r/d^2 & 0 & bx_l/d^2 & 0 \\ -by_l/d^2 & b/d & by_l/d^2 & 0 \\ -bf/d^2 & 0 & bf/d^2 & 0 \end{pmatrix} \tag{30}$$

where $d = x_l - x_r$. And $\sigma_{m_l} = diag(\sigma_x^l, \sigma_y^l)$, and $\sigma_{m_r} = diag(\sigma_x^r, \sigma_y^r)$. Where σ_x^l, σ_y^l, σ_x^r, and σ_y^r are determined by camera calibration error statistics. Usually they are in the range from 0.01 to 0.5.